MACHINE LEARNING BASED PREDICTION ON PORE FORMATION

A PREPRINT

Letian Wang
Department of Mechanical Engineering
University of California, Berkeley
Berkeley, CA, 94706
letianwang@berkeley.edu

Sara Shonkwiler
Department of Mechanical Engineering
University of California, Berkeley
Berkeley, CA, 94706
sara_shonkwiler@berkeley.edu

Bodi Yuan
Department of Mechanical Engineering
University of California, Berkeley
Berkeley, CA, 94706
bodiyuan@berkeley.edu

Sara McMain
Department of Mechanical Engineering
University of California, Berkeley
Berkeley, CA, 94706
mcmains@berkeley.edu

Jean-Baptiste Forien
Center for Engineered Materials and Manufacturing
Lawrence Livermore National Laboratory
Livermore, CA, 94550
forien1@llnl.gov

Brian Giera*
Center for Engineered Materials and Manufacturing
Lawrence Livermore National Laboratory
Livermore, CA, 94550
giera1@llnl.gov

May 2, 2019

ABSTRACT

**********TBD**********

- speed and power can provide some prediction
- pyrometer data alone have limited improvement compare to speed and power
- fixed-distance scheme is better than fixed-time scheme
- training data size have effect on the results

Keywords Machine Learning · Additive Manufacturing · Pyrometer · Defect

1 Introduction

Additive manufacturing (AM) has emerged as a revolutionary new manufacturing process. Selective Laser Melting (SLM) is a metal AM process that builds parts in layers by depositing a metal or alloy powder bed and melting the desired parts of the powder bed into track welds with a high-power laser. Metal SLM processes are used in commercial applications. For example, General Electric (GE) uses SLM to produce a jet housing part and NASA applies this process in the next-generation heavy lift rocket. As a novel manufacturing approach, SLM is prone to defects caused by minute changes in metal powder properties and laser beam parameters, as well as inherent variability in processing. The formation of pores (i.e. low density voids) decreases part strength and density of SLM components. This increases the risk of fatigue failure as the pores act as a potential site of crack initiation, which is not acceptable for aerospace applications. A systematic and high precision process monitoring system is needed to detect pores in SLM manufactured

*Corresponding Author

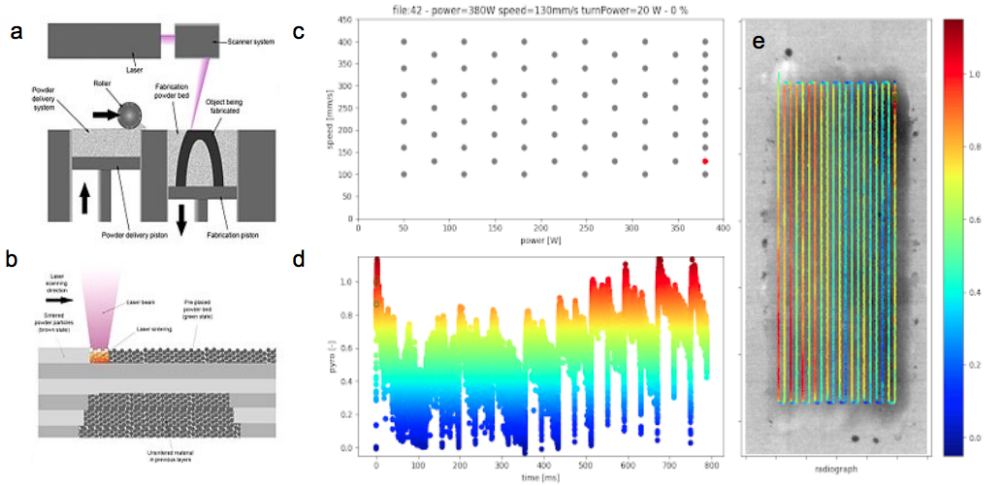

Figure 1: Experimental Setup and Data Collected.

parts. Previous process monitoring relies solely on fixed parameters and classical PID control methodologies to optimize the process.

The recent development of deep neural networks has shown great potential to integrate multidimensional data into process monitoring. A preliminary method explored in Yuan et. al. uses a CNN to monitor laser track weld quality with a high-speed camera (see Figure 1). The trained CNN successfully predicts track width, standard deviation, and continuity during each build from the in-situ video data. However, it is not able to predict the formation of pores.Furthermore, the use of a high speed camera is expensive to implement universally on SLM machines.

Hereby we prove machine learning method is effective in predicting the pore formation based on simple pyrometer data. Approaches on improving the prediction accuracy has been proposed and demonstrated.

2 Methods

2.1 Experiments and Data Sources

The experimental setup as well as the organization of data sources has been schematized in Figure 1. The pyrometer data source will be experimental measurements from the SLM machine (Aconity LAB system from Aconity3D) at Lawrence Livermore National Laboratory (LLNL). The SLM machine is equipped with a pyrometer sensor to take sensor readings. X-ray scan images of the final track welds have been manually labeled for pore location and density informations. The pyrometer sensor data with corresponding location and time are the input data, the pore number and locations are the output value. The labeled x-ray images serve as ground truth. There are over 1000 single track welds that have been manually labeled for pores. Each track weld has enough data to train a supervised deep learning algorithm. Permission and access to an appropriately sized data set has been obtained.

Power and Speed The laser head is moving at a fixed speed and power for each track. The information has been recorded in Fig.1 c.

Temperature Temperature measurement over 6 plates with around 100 tracks on each plate has been measured with pyrometer attached to the laser head. The data logging recorded the temperature, xy position of laser head as well as current time simultaneously at every 10 microseconds(Fig.1 d).

Pore The laser melted tracks are imaged with X-ray, of which the images are overlayed with temperature measurement according to the x-y location(Fig.1 e). The pore has been labeled manually on the X-ray image, which later transformed to x-y coordinates. The coordinates are poltted against the pyrometer measurement through x-y coordinate matching.

(Sara: please look into the paper describe the way we associates the pore with pyrometer data)

2.2 ML model

Features Speed and power are two stand alone parameters tested as baseline model for the ML model. Pyrometer data are the targeted feature variable for classification. Two different methods of extraction is considered.

- Fixed time: the length of input vector is defined by the time and time refresh rate of the pyrometer(100KHz)
- Fixed distance: the pyrometer data is sub-sampled in such a way that fast speed tracks meet the distance of slowest speed.

Label Two classes named as isPore and noPore is defined.

- isPore indicates the number of pores inside the investigated segment of the pyrometer data is greater than 0.
- noPore is defined as the number is 0.

Train and test set Overall 500 tracks are considered as valid data sets. The distribution of the binary classes in the total data set is 25% isPore, 75% noPore. The train size effect is investigated to confirm the quality of the data set.

Classifier and Loss function Logistic regression and cross-entropy loss is employed here for the purpose of classification. (The loss function will be modified to account for the imbalanced data set.)

Metrics The binary classification is evaluated based on the accuracy and the f1 score. Precision and recall are also plotted as supplementary items. precision and recall are defined based on the confusion matrix. The f1 score is defined

	noPore	isPore
noPore	tn	fp
isPore	fn	tp

Table 1: Confusion Metrics

as the harmonic mean of the precision and recall:

$$precision = \frac{tp}{tp + fp}, recall = \frac{tp}{tp + fn}, f1score = 2\frac{precision * recall}{precision + recall}$$

3 Results and discussion

3.1 Naive baseline model

The naive baseline model is takes on only power and speed as input feature vector. The confusion matrix is plot in Fig 2. The overall accuracy reached 83.1%, and the f1 score is 0.54. (is it good or bad?)

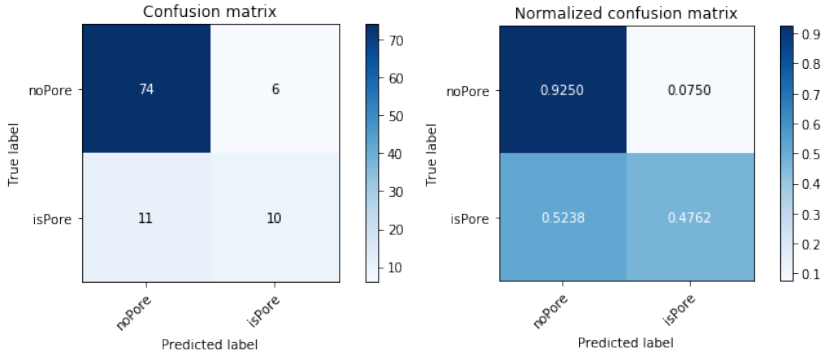

(a) Confusion Matrix

(b) Normalized Confusion Matrix

	Score
Accuracy	0.831
Precision	0.476
Recall	0.625
F1 score	0.540

(c) Metrics

Figure 2: Naive baseline model

3.2 Different schemes of pyrometer data

As specified at methods, fixed time and fixed distance schemes of extracting pyrometer data are discussed. Here we first show the hyper-parameter tuning for fixed time case. Here we see a lower performance compare to the naive model in both accuracy and f1-scores.

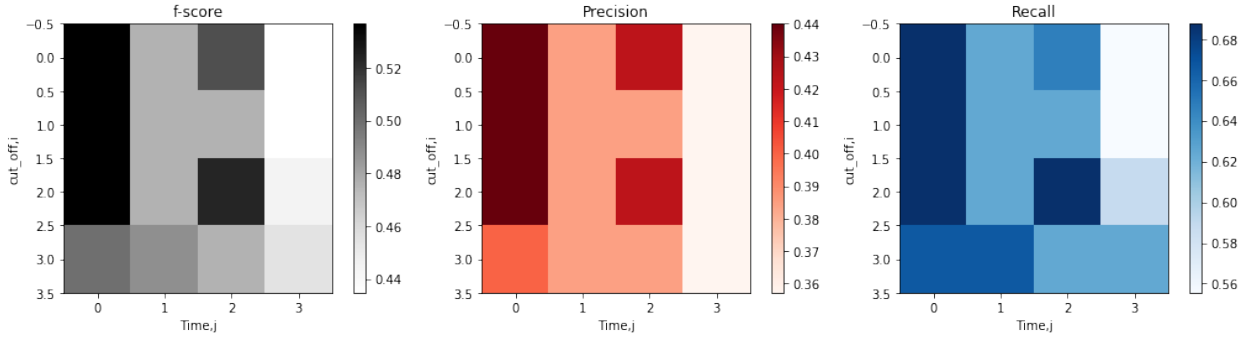

(a) F score (b) Precision (c) Recall

Figure 3: Fixed time: Metrics under different hyper-parameters

For the case of fixed distance, we did the similar hyper-parameter tuning. As a result in Fig. 4, we can see an improved precision and recall is observed in the optimized parameter set(1,1).

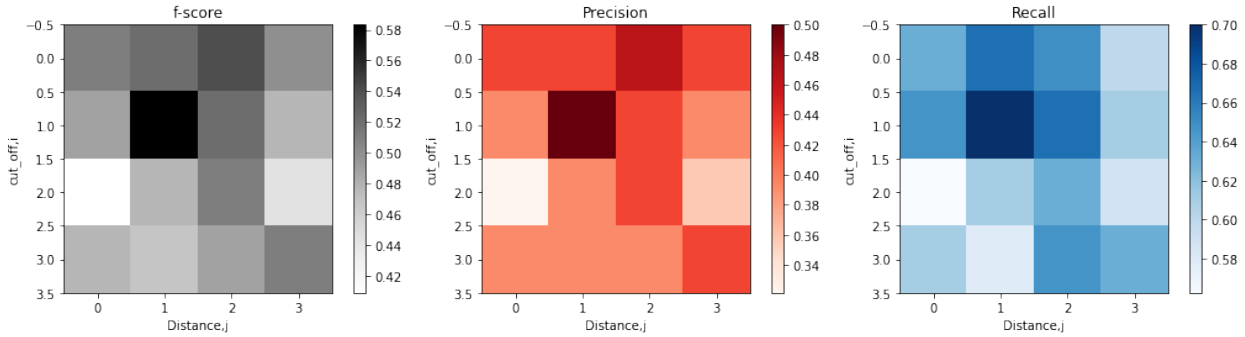

(a) F score (b) Precision (c) Recall

Figure 4: Fixed distance: Metrics under different hyper-parameters

For optimized hyper-parameters in fixed distance case, we plotted out the actual confusion matrix and resulted metric scores.As we can see in Fig.5 c, the accuracy is sacrificed to boost the f-1 score, as well as the precision and recall. (The reason should be discussed)

3.3 Training data size effect

As revealed in Fig. 6, the training data size will significantly affect the prediction metrics. We fixed the test set size to 25% of the total data sets. Then we increase the training set gradually and plotted the corresponding prediction metrics in Fig. 6. For smaller training sets, the metric is limited by the stochasticity, it is still not fully investigated. However, for larger training set, the results are more stable.

3.4 Modified loss function for the imbalanced data set

4 Conclusion

References

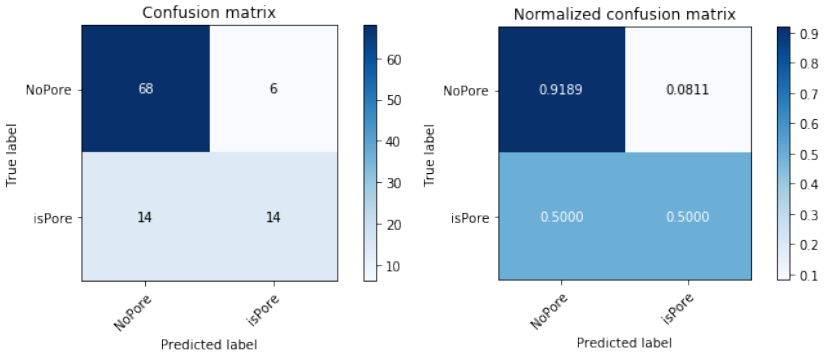

(a) Confusion Matrix

(b) Normalized Confusion Matrix

	Score
Accuracy	0.803
Precision	0.5
Recall	0.7
F1 score	0.583

(c) Metrics

Figure 5: Optmized model with only pyrometer

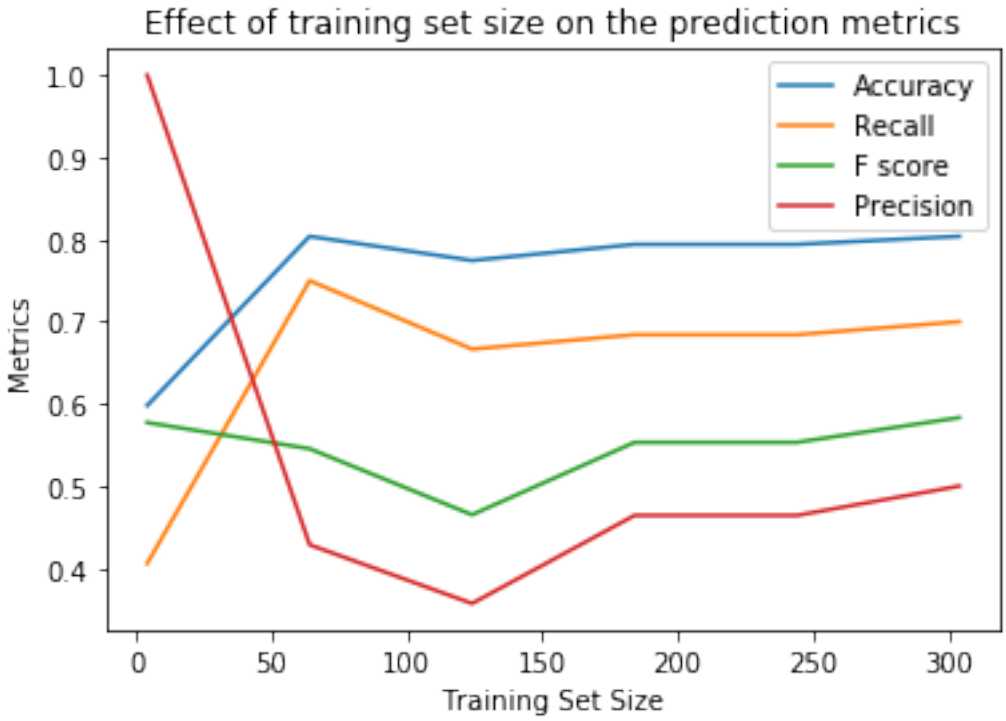

Figure 6: Effect of training set size on the prediction metrics

5 Supplementary Information

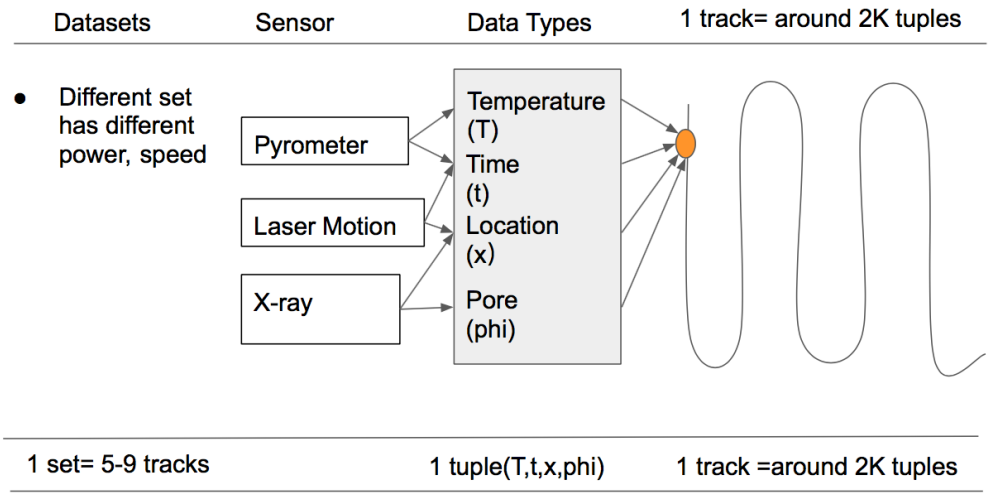

Figure 7: Data Sources